Preparation of exciplex-based fluorescent organic nanoparticles and their application in cell imaging

Xiaoyu Wang,† Lu Liu,† Shuxian Zhu, Jinghong Peng and Lidong Li [ID] *

In this paper, we report a novel organic fluorescent nanoparticle based on exciplexes for cell imaging. Through a reprecipitation method, we used a combination of 1,1-bis((di-4-tolylamino)phenyl) cyclohexane (TAPC) and 2,7-bis(diphenylphosphoryl)-9,9′-spirobi[fluorene] (SPPO13) to form nanoparticles. In the aggregated structures, TAPC and SPPO13 were forced into proximity that led to the corresponding exciplex formation. A red-shifted fluorescence emission with considerably longer fluorescence lifetimes ascribed to exciplex emission can be achieved. Along with the good stability and low cytotoxicity of organic nanoparticles, the prepared TAPC/SPPO13 exciplex nanoparticles were successfully applied in live cell imaging. These properties make TAPC/SPPO13 exciplex nanoparticles good candidates for cellular labeling and imaging materials.

Introduction

Fluorescence detection as an attractive and versatile method has been widely applied in chemical sensing and biological imaging.[1–5] An excellent fluorescence sensor depends on the optical properties of fluorescent materials themselves. Therefore, researchers have made great efforts in preparing novel small molecular dyes, conjugated polymers, quantum dots and metal clusters with satisfactory optical properties.[6–17] However, these fluorescent materials possess intrinsic emission bands. In order to meet the needs of multicolor detection, it is necessary to tune light-emission properties of fluorescent materials. The conventional method to tune light-emission properties of fluorescent materials is to change compositions and chemical structures of these materials,[18–21] which is sophisticated and time-consuming.

The emission of excimers/exciplexes usually shows a large bathochromic shift compared to that of monomers.[22–26] Excimers/exciplexes could be ideal candidates to tune and change light-emission. In concentrated solution or solid state, aromatic molecules with planar structure tend to associate with each other to form aggregates with π–π stacking interaction.[27,28] Upon irradiation, π–π stacking of associated aggregates allows charge transfer. Different species such as excimers/exciplexes may form. The excimers/exciplexes emission occurs in an unexpected energy region, which is lower than the energy of excited monomer. The red-shifted emission is assigned as a transition from excimer/exciplex state to the ground state. For example, pyrene shows an emission at 380–410 nm in molecularly

dissolved state, while in aggregated state, red-shifted emission band of pyrene at 450–500 nm appears.[29] Tuning light-emission of pyrene is realized. Thanks to a large Stokes shift (≈140 nm) and long fluorescence lifetimes (40–60 ns), pyrene excimer emission efficiently reduce the influence of the autofluorescence of biological species that facilitate fluorescent sensors.[30–32]

In the formation of excimers/exciplexes, a necessary proximity or aggregated structure is required.[33] Fluorescent organic nanoparticles (FONs) are one type of aggregated structures.[34–37] The mostly used method to prepare FONs is reprecipitation method.[38–43] By simply adding organic solution of hydrophobic fluorescent molecules into excessive poor solvent, FONs can be prepared through the self-aggregation of fluorescent molecules. The aggregated fluorophores in FONs may be expected to form excimers/exciplexes and provide a new emission. Meanwhile, FONs possess good stability in aqueous solution,[44–46] which benefits biological sensing and imaging.

In this work, we prepared a novel fluorescent organic nanoparticle based on 1,1-bis((di-4-tolylamino)phenyl)cyclohexane (TAPC) and 2,7-bis(diphenylphosphoryl)-9,9′-spirobi[fluorene] (SPPO13) *via* reprecipitation method. In the formed FONs, TAPC and SPPO13 molecules were forced into proximity. The exciplexes were formed between TAPC and SPPO13, which gave rise to a red-shifted fluorescence emission with considerably longer fluorescence lifetime. The prepared exciplex FONs exhibit a large Stokes shift, long fluorescence lifetime, good stability and low cytotoxicity, which enable the FONs to be a cell imaging material.

State Key Laboratory for Advanced Metals and Materials, School of Materials Science and Engineering, University of Science and Technology Beijing, Beijing 100083, P. R. China. E-mail: lidong@mater.ustb.edu.cn; Fax: +86-10-82375712; Tel: +86-10-82377202

† These authors contributed equally.

Experimental

Materials

TAPC was purchased from Tokyo Chemical Industry and SPPO13 was purchased from Luminescence Technology Corp.

Tetrahydrofuran (THF) was purchased from Beijing Chemical Works and distilled from Na/diphenylketone. Other inorganic salts and organic solvents were purchased from Sigma-Aldrich and used without further purification. MCF-7 breast cancer cells were purchased from cell culture center of Institute of Basic Medical Sciences, Chinese Academy of Medical Sciences (Beijing, China). Ultrapure Millipore water (18.6 $M\Omega$) was used throughout the experiments.

Measurements

The average hydrodynamic diameters were measured with a Nano ZS90 instrument (Malvern Instrument Ltd., England) based on dynamic light scattering (DLS) technique. The morphology of the nanoparticles was characterized by scanning electron microscope (SEM, Carl Zeiss Jena, SUPRA 55 SAPPHIRE). Fluorescence spectra and excitation spectra were measured with a Hitachi F-7000 fluorescence spectrometer equipped with a xenon lamp as the light source. Fluorescence photographs of exciplex FONs were captured by a Nikon D-7000 camera. The absolute fluorescence quantum yields were measured with an absolute photoluminescence quantum yield measurement system (Hamamatsu C11347). Time-domain lifetime measurements were performed by an Edinburgh Instruments F900 spectrometer with excitation at 266 nm. Fluorescence microscopy images of cells were obtained using an Olympus 1X73 fluorescence microscopy with mercury lamp as the light source. Cell viability was recorded with a Spectra MAX 340PC plate reader. The pH values of the solutions were measured by a pH meter.

Preparation of TAPC/SPPO13 exciplex FONs

In our experiments, TAPC and SPPO13 were separately dissolved in THF with a concentration of 2 mg mL^{-1}. 100 μL of TAPC solution and 50 μL of SPPO13 solution were mixed fully and then rapidly injected into 1 mL of deionized water to form TAPC/SPPO13 exciplex FONs. As control groups, TAPC and SPPO13 nanoparticles were prepared via the same method, respectively.

Stability assay of the TAPC/SPPO13 exciplex FONs

To evaluate the stability of nanoparticles, 100 μL of TAPC/SPPO13 exciplex FONs were dispersed in 1 mL of different pH solution (pH = 5.8, 6.4, 7.1, 8.3, 9.7), phosphate buffered saline (PBS, pH = 7.4) and Dulbecco's modified Eagle's medium (DMEM) containing 10% FBS (v/v). The pH values of the solutions were adjusted using either 1 M HCl or 1 M NaOH. The fluorescence spectrum of each sample was measured after 10 min of equilibrium.

Cellular imaging for the TAPC/SPPO13 exciplex FONs

MCF-7 breast cancer cells were cultured in DMEM containing 10% FBS (v/v) and then seeded on 35×35 mm culture plates, incubated at 37 °C in a 5% CO_2 humidified atmosphere for 24 h. The medium was replaced by 1 mL culture medium (DMEM containing 10% FBS (v/v)) containing 100 μL of TAPC/SPPO13 exciplex FONs. After the plate was incubated at 37 °C in a 5% CO_2 humidified atmosphere for 10 h, the cells were washed three times using PBS. Fluorescence microscopy images and phase contrast bright-field images were recorded on an Olympus 1X73 fluorescence microscopy with mercury lamp as the light source. The fluorescence microscopy images were recorded using a 375/28 nm excitation filter with 100 ms exposure time.

In vitro cell viability assay of the TAPC/SPPO13 exciplex FONs

The cytotoxicity of TAPC/SPPO13 exciplex FONs was evaluated by the 3-(4,5-dimethylthiazol-2-yl)-2,5-diphenyltetrazolium bromide (MTT) method. MCF-7 cells were seeded into 96-well plates maintained overnight in DMEM containing 10% FBS (v/v) at 37 °C in a 5% CO_2 humidified atmosphere. And then MCF-7 cells were treated with various concentrations of TAPC/SPPO13 exciplex FONs for 24 h. The concentration of TAPC/SPPO13 exciplex FONs was determined using the concentration of TAPC. TAPC concentration is changed from 0 to 40 $\mu g\ mL^{-1}$. Subsequently, 100 μL of MTT (1 mg mL^{-1} in culture medium) was added to each well with further incubation at 37 °C for 4 h after the medium was removed. After that, we discarded the supernatant, added 100 μL of DMSO per well. The plate was gently shaken for 5 min. The absorbance values of purple formazan were recorded at 570 nm using a Spectra MAX 340PC plate reader. The cell viability was expressed by the ratio of the absorbance of the cells incubated with various concentrations of TAPC/SPPO13 exciplex FONs to that of the cells incubated with culture medium only.

Results and discussion

It is well known that the planar structures of molecules play the most important role in the excimers/exciplexes formation.[47,48] Here we selected TAPC and SPPO13 molecules to form exciplexes. The chemical structures of TAPC and SPPO13 were shown in Fig. 1a. TAPC contains two planar triphenylamine groups and SPPO13 contains planar fluorene groups, which provide considerable probability for exciplexes formation. A combination of TAPC and SPPO13 was used to prepare TAPC/SPPO13 FONs. Due to the hydrophobic properties of TAPC and SPPO13, TAPC, SPPO13 and TAPC/SPPO13 nanoparticles were prepared through the reprecipitation process, respectively. By DLS measurements, we studied the formation of nanoparticles in aqueous solutions. The average of hydrodynamic diameter of the TAPC, SPPO13 and TAPC/SPPO13 nanoparticles were measured to be 175.0 ± 5.8 nm, 112.6 ± 5.8 nm and 130.4 ± 7.1 nm, respectively. Scanning electron microscopy (SEM) was further used to characterize the morphology and size of these nanoparticles. As shown in Fig. 1b–d, TAPC, SPPO13 and TAPC/SPPO13 nanoparticles were indeed formed in aqueous solution. All of these nanoparticles have spherical morphology and highly uniform size. The diameters of TAPC, SPPO13 and TAPC/SPPO13 nanoparticles are measured to be 165 ± 3 nm, 107 ± 17 nm and 121 ± 11 nm, respectively.
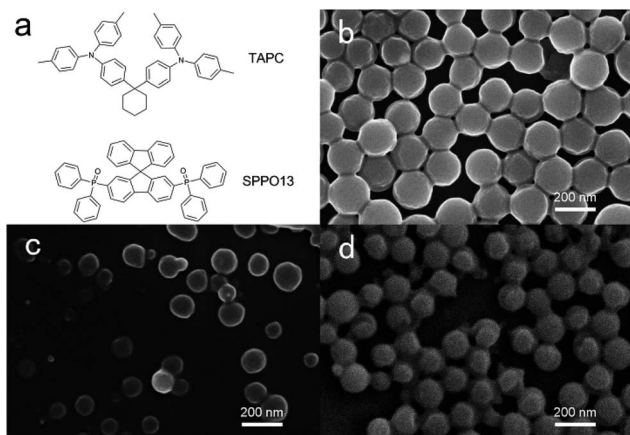
Fig. 1 (a) Chemical structures of TAPC and SPPO13. SEM images of (b) TAPC, (c) SPPO13 and (d) TAPC/SPPO13 nanoparticles. The scale bar represents 200 nm.

Then, we measured the emission spectra of three nanoparticles. As shown in Fig. 2, TAPC nanoparticles only display their monomer emission at around 379 nm and SPPO13 nanoparticles display their monomer emission at around 377 nm. However, TAPC/SPPO13 nanoparticles display an intense long-wavelength emission band at 477 nm together with a weak emission at 378 nm. The absolute fluorescence quantum yields of TAPC, SPPO13 and TAPC/SPPO13 nanoparticles were measured to be 7.6%, 5.2% and 15.0%, respectively. As the emission quantum yield of TAPC/SPPO13 nanoparticles is higher than the other two nanoparticles, the bright fluorescence of TAPC/SPPO13 nanoparticles could be visually observed (inset in Fig. 2), which benefit biological imaging. A large Stokes shift ($\approx$170 nm) was observed for TAPC/SPPO13 nanoparticles. The emission band at short wavelength arises from the native emission from the monomers. We infer that the new emission

at 477 nm might originate from exciplexes that were formed by TAPC and SPPO13. This is because TAPC contains planar triphenylamine groups and SPPO13 contains planar fluorene groups. In the formed nanoparticles, TAPC and SPPO13 were forced into proximity to form π–π stacking structures. Meanwhile, the electron-rich triphenylamine groups in TAPC have a higher affinity for electron-poor triphenylphosphine groups in SPPO13, which further benefit the close overlap between the planar triphenylamine and fluorene. Thus, electron transfer between TAPC and SPPO13 facilely occurred and exciplexes formed. As the corresponding photon energy of the emission peak at 477 nm is evaluated to be 2.6 eV, which is almost equivalent to the energy difference between highest occupied molecular orbital (HOMO) of TAPC[49] and lowest unoccupied molecular orbital (LUMO) of SPPO13 (ref. 50) (Fig. 3). The new emission at 477 nm can be attributed to the exciplex emission.

In order to verify the new emission band of the TAPC/SPPO13 nanoparticles originate from exciplex emission, we compared the fluorescence excitation spectra of TAPC/SPPO13 nanoparticles with neat TAPC nanoparticles. As shown in Fig. 4a, the excitation spectrum of TAPC/SPPO13 nanoparticles is very similar to that of TAPC nanoparticles. The result indicates that the new emission of the TAPC/SPPO13 nanoparticles arises from the same excitation pathway with TAPC. Depending on the relative proximity between TAPC and SPPO13, unique monomer and excimer emissions are observed at considerably different wavelengths. We then examined the emission spectrum of solution containing TAPC and SPPO13 nanoparticles. As shown in Fig. 4b, exciplex emission does not appear in the binary nanoparticles solution, where TAPC and SPPO13 molecules have larger distances than them in the TAPC/SPPO13 nanoparticles. These results confirm that the new emission band results from exciplexes formed in TAPC/SPPO13 nanoparticles. In the TAPC/SPPO13 nanoparticles, two kinds of molecules are forced into proximity which required for the formation of the excited-state dimers. Thus, TAPC/SPPO13 exciplex FONs were
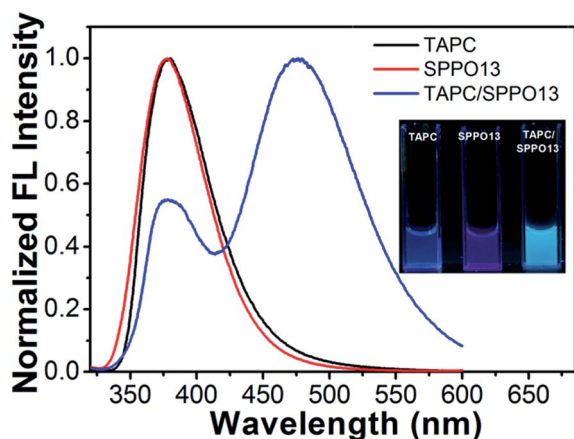

Fig. 2 Normalized emission spectra of TAPC, SPPO13 and TAPC/SPPO13 nanoparticles, respectively. The excitation wavelength was 300 nm for TAPC and TAPC/SPPO13 nanoparticles, and 282 nm for SPPO13 nanoparticles. Inset: fluorescence photographs of TAPC, SPPO13 and TAPC/SPPO13 nanoparticles following irradiation at 365 nm.
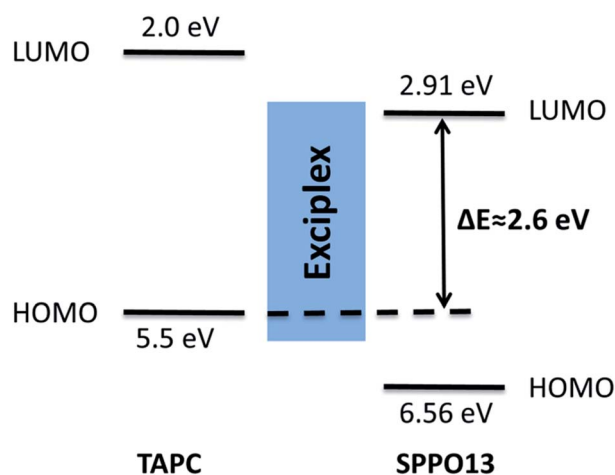

Fig. 3 Influence of the LUMO level of SPPO13 and HOMO level of TAPC on the exciplex emission energy. ΔE denotes the energy gap between the LUMO level of SPPO13 and HOMO level of TAPC.

Fig. 5   Fluorescence intensity decay of emission at 378 nm and 477 nm for TAPC/SPPO13 nanoparticles at room temperature.
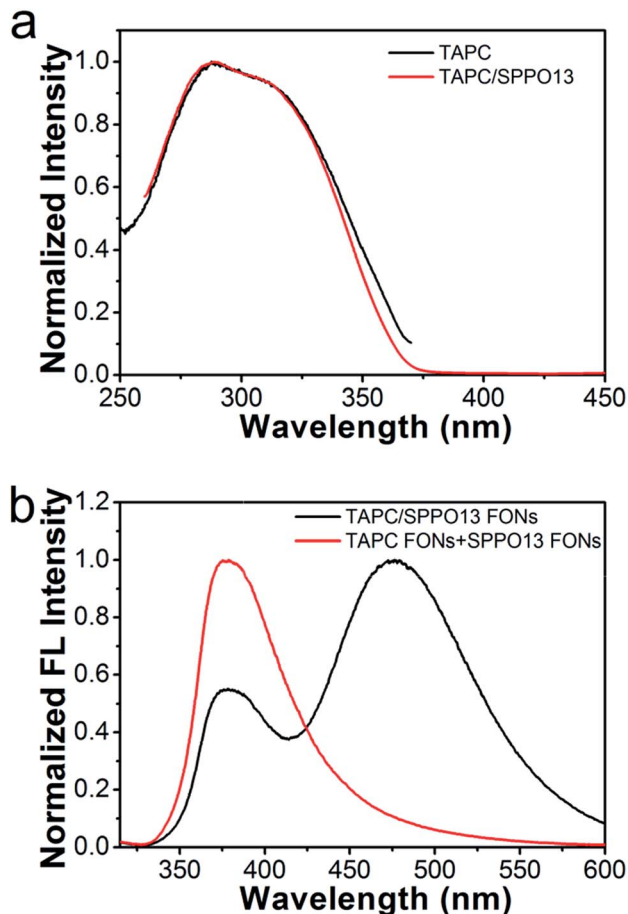
Fig. 4   (a) Normalized excitation spectra of TAPC and TAPC/SPPO13 nanoparticles. (b) Normalized emission spectra of TAPC/SPPO13 nanoparticles and the mixture of TAPC nanoparticles and SPPO13 nanoparticles. The excitation wavelength was 300 nm.

Table 1   Exponential components analysis of the fluorescence intensity decay of TAPC/SPPO13 exciplex FONs with the time-correlated single-photon counting technique

	B_i	τ_i (ns)	f_i	χ^2	$\langle\tau\rangle$ (ns)
378 nm	0.0299	0.718	45.957%	1.510	2.44
	0.0065	3.894	54.043%		
477 nm	2188.7	4.873	4.126%	1.049	321.42
	398.55	54.392	8.386%		
	624.64	362.054	87.488%		

obtained, and the light-emission of nanoparticles has been tuned.

Since the formation of excited-state dimers involving molecular interactions, the excimer state possesses relatively longer lifetime than the monomer state.[51] We investigated the fluorescence intensity decays for TAPC/SPPO13 exciplex FONs (Fig. 5). The decay time of the exciplex states at 477 nm is obviously longer than that detected at the monomer emission at 378 nm, which further demonstrates the formation of exciplexes. The intensities of TAPC/SPPO13 exciplex FONs show multiexponential decays. The fitted parameters for intensity decays were displayed in Table 1. B values are called the preexponential factors and τ values are characteristic lifetimes. The calculated average lifetime for monomer emission is 2.44 ns according to Table 1, while the calculated average lifetime for exciplex emission is 321 ns. The lifetime for exciplex emission is long enough to prevent any influence of the autofluorescence of biological species in biological imaging. This property allows TAPC/SPPO13 exciplex FONs to act as a fluorescent probe for biological imaging.

The TAPC/SPPO13 exciplex FONs offer the advantage of a large Stokes shift and long fluorescence lifetime, the stability
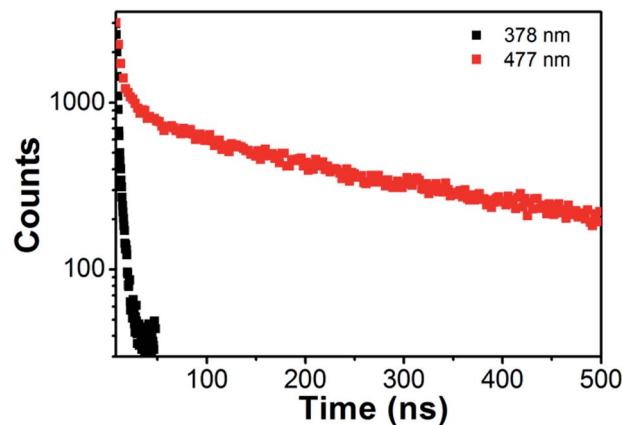
of the nanocomposites in different solution also need to be investigated for their further application in cell imaging. During rapid growing of cancer cells, high rate of glycolysis under both aerobic and anaerobic conditions result in the accumulation of lactic acid. It leads to acidic pH in tumor tissues.[52] As shown in Fig. 6a, the emission spectra of TAPC/SPPO13 exciplex FONs are almost unchanged over the wide pH range from 5.8 to 9.7. And the exciplex emission is slightly changed in the PBS and cell culture medium (DMEM containing 10% FBS (v/v)) (Fig. 6b). Thus, the TAPC and SPPO13 molecules still keep close contact in different solution. The TAPC/SPPO13 exciplex FONs possess good stability in different solution that benefits biological imaging.

Finally, the TAPC/SPPO13 exciplex FONs were applied for cellular imaging. MCF-7 breast cancer cells were incubated with the nanoparticles for 10 h at 37 °C and washing twice with PBS buffer. Fig. 7 shows the image of MCF-7 cells before and after incubation with TAPC/SPPO13 nanoparticles. No fluorescent signal is observed from the MCF-7 cells before incubation with nanoparticles (Fig. 7a). After incubation with TAPC/SPPO13 exciplex FONs, strong blue fluorescence is observed from the MCF-7 cells (Fig. 7b). The overlap image of phase contrast and fluorescence image of MCF-7 cells shows that the nanoparticles could be internalized by the cells (Fig. 7c and d). They were uniformly located in the cytoplasm and around the nucleus. This observation indicates that the exciplex FONs have potential application in cell imaging.
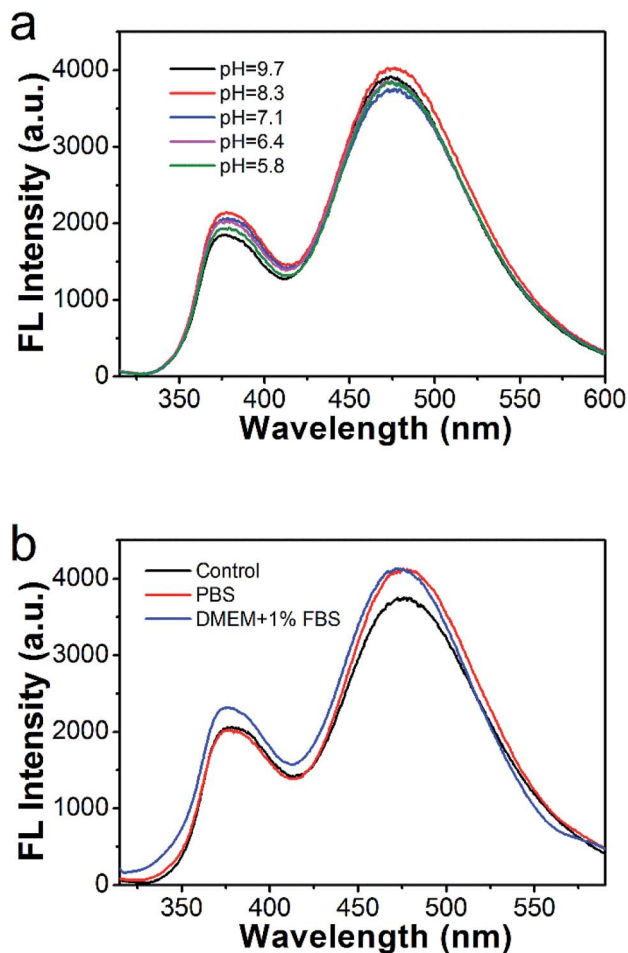
Fig. 6 (a) Emission spectra for TAPC/SPPO13 nanoparticles as a function of different pH. (b) Emission spectra for TAPC/SPPO13 nanoparticles in PBS and cell culture medium. The control group is the TAPC/SPPO13 nanoparticles in water. The excitation wavelength was 300 nm.

Fig. 7 (a) Fluorescent microscopy images of MCF-7 cells before incubation with TAPC/SPPO13 nanoparticle. (b) Fluorescent micros-copy images, (c) phase contrast and (d) the overlap image of phase contrast and fluorescence image of MCF-7 cells after incubation with TAPC/SPPO13 nanoparticle. The scale bar represents 5 μm.

Fig. 8 Cell viability results of MCF-7 cells after incubation with various TAPC/SPPO13 nanoparticles concentration.

For the cellular labeling and imaging materials, cytotoxicity is an important factor that should be considered. So we investigated the cytotoxicity of the TAPC/SPPO13 exciplex FONs, using a MTT cell-viability assay. Because the cell viability is proportional to the absorption of produced for-mazan at 570 nm, the cell viability was calculated as the ratio of the absorbance of the cells incubated with TAPC/SPPO13 exciplex FONs to that of the cells incubated with culture medium only. In our experiment, the concentration of TAPC/SPPO13 exciplex FONs was determined by the concentration of TAPC. In the TAPC concentration range from 5 μg mL^{-1} to 40 μg mL^{-1}, the relative cell viabilities were more than 94% after incubation of MCF-7 cells with various concentrations of TAPC/SPPO13 exciplex FONs for 24 h (Fig. 8). At a TAPC concentration of 20 μg mL^{-1} which used in cell imaging experiment, the relative cell viability is more than 100%. The results indicate that the TAPC/SPPO13 exciplex FONs display low cytotoxicity. They can be used as biocompatible probes for cell imaging application.
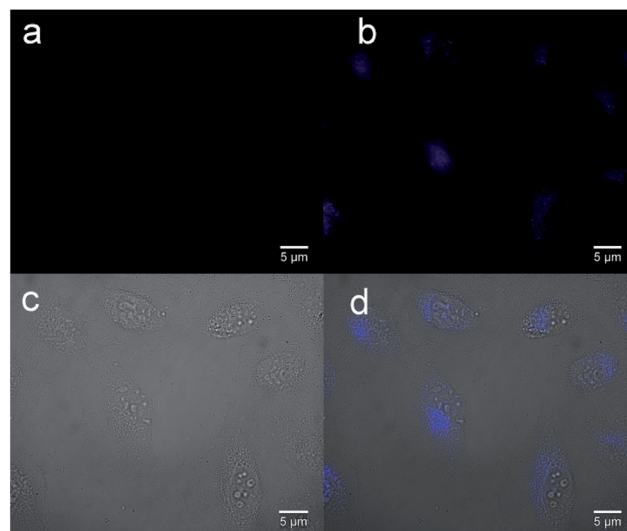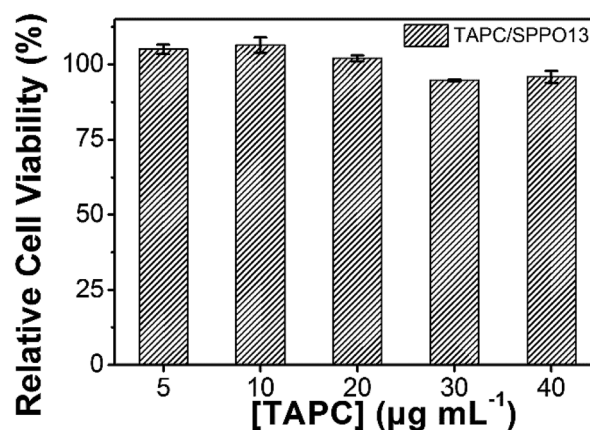
Conclusions

In summary, we have developed a novel fluorescent organic nanoparticle based on TAPC/SPPO13 exciplexes for cell imaging. In the nanoparticle system, the close contact between TAPC and SPPO13 leads to the formation of excited-state dimers and the corresponding exciplex emission. A large Stokes shift of 170 nm and a long fluorescence lifetime of 321 ns have been observed in TAPC/SPPO13 exciplex FONs. These properties are suitable for efficient cellular imaging. Moreover, the good stability and low cytotoxicity of TAPC/SPPO13 exciplex FONs greatly potentiate their application in cell imaging. We there-fore believe that these exciplex FONs have great potential as fluorescent materials for biological imaging.

Conflicts of interest

There are no conflicts to declare.

Acknowledgements

Notes and references

1 M. E. Tanenbaum, L. A. Gilbert, L. S. Qi, J. S. Weissman and R. D. Vale, *Cell*, 2014, **159**, 635–646.

2 T. Kowada, H. Maeda and K. Kikuchi, *Chem. Soc. Rev.*, 2015, **44**, 4953–4972.

3 C. Zhu, L. Liu, Q. Yang, F. Lv and S. Wang, *Chem. Rev.*, 2012, **112**, 4687–4735.

4 U. H. F. Bunz, K. Seehafer, M. Bender and M. Porz, *Chem. Soc. Rev.*, 2015, **44**, 4322–4336.

5 X. Wang, S. Li, P. Zhang, F. Lv, L. Liu, L. Li and S. Wang, *Adv. Mater.*, 2015, **27**, 6040–6045.

6 A. L. Antaris, H. Chen, K. Chen, Y. Sun, G. Hong, C. Qu, S. Diao, Z. Deng, X. Hu, B. Zhang, X. Zhang, O. K. Yaghi, Z. R. Alamparambil, X. Hong, Z. Cheng and H. Dai, *Nat. Mater.*, 2016, **15**, 235–242.

7 S. He, B. Song, D. Li, C. Zhu, W. Qi, Y. Wen, L. Wang, S. Song, H. Fang and C. Fan, *Adv. Funct. Mater.*, 2010, **20**, 453–459.

8 E. H. Hill, Y. Zhang, D. G. Evans and D. G. Whitten, *ACS Appl. Mater. Interfaces*, 2015, **7**, 5550–5560.

9 X. Wang, Q. Cui, C. Yao, S. Li, P. Zhang, H. Sun, F. Lv, L. Liu, L. D. Li and S. Wang, *Adv. Mater. Technol.*, 2017, **2**, 1700033.

10 S. Rochat and T. M. Swager, *J. Am. Chem. Soc.*, 2013, **135**, 17703–17706.

11 X. Feng, L. Liu, S. Wang and D. Zhu, *Chem. Soc. Rev.*, 2010, **39**, 2411–2419.

12 C. F. Calver, K. S. Schanze and G. Cosa, *ACS Nano*, 2016, **10**, 10598–10605.

13 Q. Cui, J. Xu, X. Wang, L. Li, M. Antonietti and M. Shalom, *Angew. Chem., Int. Ed.*, 2016, **55**, 3672–3676.

14 X.-D. Zhang, Z. Luo, J. Chen, X. Shen, S. Song, Y. Sun, S. Fan, F. Fan, D. T. Leong and J. Xie, *Adv. Mater.*, 2014, **26**, 4565–4568.

15 H. Kobayashi, M. Ogawa, R. Alford, P. L. Choyke and U. Yasuteru, *Chem. Rev.*, 2010, **110**, 2620–2640.

16 H. Wang, J. Liu, A. Han, N. Xiao, Z. Xue, G. Wang, J. Long, D. Kong, B. Liu, Z. Yang and D. Ding, *ACS Nano*, 2014, **8**, 1475–1484.

17 D. Mao, J. Liu, S. Ji, T. Wang, Y. Hu, D. Zheng, R. Yang, D. Kong and D. Ding, *Biomaterials*, 2017, **143**, 109–119.

18 P. L. Donabedian, M. N. Creyer, F. A. Monge, K. S. Schanze, E. Y. Chi and D. G. Whitten, *Proc. Natl. Acad. Sci. U. S. A.*, 2017, **114**, 7278–7282.

19 Q. Cui, X. Wang, Y. Yang, S. Li, L. Li and S. Wang, *Chem. Mater.*, 2016, **28**, 4661–4669.

20 H.-W. Mo, Y. Tsuchiya, Y. Geng, T. Sagawa, C. Kikuchi, H. Nakanotani, F. Ito and C. Adachi, *Adv. Funct. Mater.*, 2016, **26**, 6703–6710.

21 Y. Huang, E. J. Kramer, A. J. Heeger and G. C. Bazan, *Chem. Rev.*, 2014, **114**, 7006–7043.

22 M. Son, K. H. Park, C. Shao, F. Würthner and D. Kim, *J. Phys. Chem. Lett.*, 2014, **5**, 3601–3607.

23 C. Wei, M. Gao, F. Hu, J. Yao and Y. Zhao, *Adv. Opt. Mater.*, 2016, **4**, 1009–1014.

24 D. Kraskouskaya, M. Bancerz, H. S. Soor, J. E. Gardiner and P. T. Gunning, *J. Am. Chem. Soc.*, 2014, **136**, 1234–1237.

25 X. Xu, Z. Xu, S. Ye, Y. Liu, M. Wu and L. Li, *Part. Part. Syst. Charact.*, 2015, **32**, 962–969.

26 P. Conlon, C. J. Yang, Y. Wu, Y. Chen, K. Martinez, Y. Kim, N. Stevens, A. A. Marti, S. Jockusch, N. J. Turro and W. Tan, *J. Am. Chem. Soc.*, 2008, **130**, 336–342.

27 D. Kim and J. L. Brédas, *J. Am. Chem. Soc.*, 2009, **131**, 11371–11380.

28 T. Nakano, K. Takewaki, T. Yade and Y. Okamoto, *J. Am. Chem. Soc.*, 2001, **123**, 9182–9183.

29 C. E. Agudelo-Morales, R. E. Galian and J. Pérez-Prieto, *Anal. Chem.*, 2012, **84**, 8083–8087.

30 J. Huang, Y. Wu, Y. Chen, Z. Zhu, X. Yang, C. Yang, K. Wang and W. Tan, *Angew. Chem., Int. Ed.*, 2011, **50**, 401–404.

31 Y. Wu, J. Wang, F. Zeng, S. Huang, J. Huang, H. Xie, C. Yu and S. Wu, *ACS Appl. Mater. Interfaces*, 2016, **8**, 1511–1519.

32 M. Fischbach, U. Resch-Genger and O. Seitz, *Angew. Chem., Int. Ed.*, 2014, **53**, 11955–11959.

33 K. E. Brown, W. A. Salamant, L. E. Shoer, R. M. Young and M. R. Wasielewski, *J. Phys. Chem. Lett.*, 2014, **5**, 2588–2593.

34 X. Wang, L. Liu, S. Zhu and L. Li, *Colloids Surf., A*, 2017, **520**, 72–77.

35 C.-C. Shih, Y.-C. Chiu, W.-Y. Lee, J.-Y. Chen and W.-C. Chen, *Adv. Funct. Mater.*, 2015, **25**, 1511–1519.

36 Y. Yang, X. Wang, Q. Cui, Q. Cao and L. Li, *ACS Appl. Mater. Interfaces*, 2016, **8**, 7440–7448.

37 C. Wu and D. T. Chiu, *Angew. Chem., Int. Ed.*, 2013, **52**, 3086–3109.

38 M. Wu, X. Xu, J. Wang and L. Li, *ACS Appl. Mater. Interfaces*, 2015, **7**, 8243–8250.

39 C. Szymanski, C. Wu, J. Hooper, M. A. Salazar, A. Perdomo, A. Dukes and J. McNeill, *J. Phys. Chem. B*, 2005, **109**, 8543–8546.

40 S. Li, X. Wang, R. Hu, H. Chen, M. Li, J. Wang, Y. Wang, L. Liu, F. Lv, X.-J. Liang and S. Wang, *Chem. Mater.*, 2016, **28**, 8669–8675.

41 H. Yuan, L. Wang, S. Li, H. Liang, C. Lu, Y. Wang and C.-H. Zhao, *J. Mater. Chem. B*, 2016, **4**, 5515–5518.

42 K. Y. Pu, A. J. Shuhendler, J. V. Jokerst, J. G. Mei, S. S. Gambhir, Z. N. Bao and J. H. Rao, *Nat. Nanotechnol.*, 2014, **9**, 233–239.

43 A. D'Aléo, A. Felouat, V. Heresanu, A. Ranguis, D. Chaudanson, A. Karapetyan, M. Giorgi and F. Fages, *J. Mater. Chem. C*, 2014, **2**, 5208–5215.

44 X. Wang, F. He, L. Li, H. Wang, R. Yan and L. Li, *ACS Appl. Mater. Interfaces*, 2013, **5**, 5700–5708.

45 L. Feng, C. Zhu, H. Yuan, L. Liu, F. Lv and S. Wang, *Chem. Soc. Rev.*, 2013, **42**, 6620–6633.

46 X. Xu, R. Liu and L. Li, *Chem. Commun.*, 2015, **51**, 16733–16749.

47 I. Prieto, J. Teetsov, M. A. Fox, D. A. Vanden Bout and A. J. Bard, *J. Phys. Chem. A*, 2001, **105**, 520–523.

48 S. A. Bagnich, S. Athanasopoulos, A. Rudnick, P. Schroegel, I. Bauer, N. C. Greenham, P. Strohriegl and A. Köhler, *J. Phys. Chem. C*, 2015, **119**, 2380–2387.

49 V. Jankus, P. Data, D. Graves, C. McGuinness, J. Santos, M. R. Bryce, F. B. Dias and A. P. Monkman, *Adv. Funct. Mater.*, 2014, **24**, 6178–6186.

50 S. O. Jeon and J. Y. Lee, *J. Mater. Chem.*, 2012, **22**, 4233–4243.

51 Y. Kim, J. Bouffard, S. E. Kooi and T. M. Swager, *J. Am. Chem. Soc.*, 2005, **127**, 13726–13731.

52 O. Onaca, R. Enea, D. W. Hughes and W. Meier, *Macromol. Biosci.*, 2009, **9**, 129–139.